

Multiobjective Topology Optimization of a Beam Under Torsion and Distortion

Tae Soo Kim* and Yoon Young Kim†
Seoul National University, Seoul 151-742, Republic of Korea

The objective is to present multiobjective topology optimization for the design of a thin-walled beam section. Unlike existing reports on beam-section optimization, the present study takes into account a distortional rigidity in addition to a torsional rigidity. To alleviate the conflict in maximization of the torsional and distortional rigidities, the use of a multiobjective function in product form is suggested. We also propose to use the eigenvalue of the in-plane stiffness matrix of a general beam section in representing the distortional rigidity.

I. Introduction

BEAM-SECTION optimization has been one of the interesting topics in the field of structural optimization. Because beams under bending or torsional loads are common, most work on the beam-section optimization has been concerned with bending or torsional rigidity maximization. To achieve this goal, earlier attempt was made by analytic methods.^{1,2} As numerical methods, such as finite elements and boundary elements, become powerful tools for structural optimization, the design problems of more general cross sections have been worked out.^{3,4} However, they have investigated the design of simply connected cross sections only; complex and practical cross sections have not been considered.

To overcome the limitation just mentioned, Kim and Kim⁵ have recently proposed a new approach based on topology optimization. This work demonstrates that a thin-walled section can be obtained as an optimal solution when the mass constraint of the topology optimization problem becomes tight. It is also pointed out that the torsional rigidity alone can be used as a design objective because the torsional rigidity is always smaller than the mean bending rigidity. In the case of thin-walled beams under general loading, however, cross sections might be distorted significantly near loaded ends.^{6,7} To prevent such distortional deformations, the distortional rigidity of a beam section needs to be considered in addition to the torsional rigidity.

In the present work beam-section topology optimization is formulated to find an optimal thin-walled section having appropriate torsional and distortional rigidities. The torsional rigidity of a general cross section can be derived from the well-known Saint Venant torsion problem.⁸ The distortional rigidity of a general cross section has not been defined so far, although an explicit definition for the case of thin-walled sections can be found in Ref. 7. Extending the notion of the distortional stiffness in Ref. 7, we represent the distortional rigidity of general cross sections by the fundamental eigenvalue of the in-plane stiffness matrix of the cross section. The major difficulty in the present multiobjective problem is that maximizing the torsional rigidity alone yields a thin-walled hollow section, whereas maximizing the distortional rigidity alone yields a lumped mass concentrated at the center of a cross section. To compromise the conflicting nature of the rigidities, a multiobjective function in product form is proposed. The advantage of the present

multiobjective function is that it has balanced sensitivities between objectives. Numerical examples show that the present multiobjective function has superior convergence performance to typical multiobjective functions in the form of weighted sums.

II. Formulation of Beam-Section Topology Optimization

Topology optimization, proposed by Bendsøe and Kikuchi,⁹ is a framework in which the optimal material distribution of an elastic body satisfying given design requirements is sought. Finding the optimal on-off distribution of a material is originally an ill-posed problem. The basic idea of the homogenization approach to topology optimization lies in the relaxation of this ill-posed problem using a microstructure. To evaluate the macroscopic property of the microstructure, a homogenization method is employed. However, the present work employs a power law approach,^{10,11} which has been proven physically realizable for certain powers.¹² Before considering multiobjective topology optimization, we consider the topology optimization formulation either for the maximization of the torsional rigidity or for the distortional rigidity.

A. Torsional Rigidity Maximization

Following the procedure in Ref. 5, the beam-section topology optimization problem to maximize the torsional rigidity can be stated as follows:

Minimize

$$f(\rho) = -D_t(\rho) \quad (1a)$$

such that

$$h(\rho) = \sum_{e=1}^{N_e} \int_{A_e} \rho_e \, dA - M_0 = 0 \quad (1b)$$

$$\rho_l \leq \rho_e \leq \rho_u \quad (1c)$$

where

$$\rho = \{\rho_e\}^T, \quad e = 1, 2, \dots, N_e \quad (1d)$$

The allowed beam section mass is specified by M_0 , and the total number of finite elements used to discretize the cross section is denoted by N_e . The design variable ρ_e is the material density of the e th finite element. The lower (ρ_l) and upper (ρ_u) bounds on the design variables are taken as $\rho_l = 0.01$ and $\rho_u = 1.0$ in the present work.

The torsional rigidity $D_t(\rho)$ in Eq. (1a) can be constructed from the discretized form of the original definition in Eq. (2):

$$D_t = 2 \int_A \phi(x, y) \, dA \quad (2)$$

Received 30 June 2000; revision received 15 April 2001; accepted for publication 17 April 2001. Copyright © 2001 by Tae Soo Kim and Yoon Young Kim. Published by the American Institute of Aeronautics and Astronautics, Inc., with permission. Copies of this paper may be made for personal or internal use, on condition that the copier pay the \$10.00 per-copy fee to the Copyright Clearance Center, Inc., 222 Rosewood Drive, Danvers, MA 01923; include the code 0001-1452/02 \$10.00 in correspondence with the CCC.

*Graduate Student, School of Mechanical and Aerospace Engineering, Shinlim-Dong, San 56-1, Kwanak-Gu.

†Professor, School of Mechanical and Aerospace Engineering, Shinlim-Dong, San 56-1, Kwanak-Gu.

where the Prandtl stress function $\phi(x, y)$ satisfies the following equation:

$$\frac{\partial}{\partial x} \left[\frac{1}{G(x, y)} \frac{\partial \phi(x, y)}{\partial x} \right] + \frac{\partial}{\partial y} \left[\frac{1}{G(x, y)} \frac{\partial \phi(x, y)}{\partial y} \right] = -2 \quad (3)$$

Equation (3) is the governing equation of the Saint Venant torsion problem, where x and y denote the Cartesian coordinates, and $G(x, y)$ is the shear modulus. The detailed derivation of Eqs. (2) and (3) can be found in Ref. 8.

A discretized form of Eq. (2) can be put into

$$D_t(\rho) = \Phi^T \phi K \Phi \quad (4)$$

where ϕK is the stiffness matrix of Eq. (3) and Φ denotes the nodal value array of the stress function $\phi(x, y)$. In the topology optimization setting the design variable ρ_e controls the stiffness matrix as

$$\phi K = \sum_{e=1}^{N_e} \int_{A_e} \phi B_e^T \phi D(\rho_e) \phi B_e \, dA \quad (5)$$

where

$$\phi D(\rho_e) = \frac{1}{G(\rho_e)} \begin{pmatrix} 1 & 0 \\ 0 & 1 \end{pmatrix}, \quad G(\rho_e) = G_0 \left(\frac{\rho_e}{\rho_u} \right)^n \quad (6)$$

The symbol ϕB_e in Eq. (5) is the interpolation matrix for the derivatives of Φ in an element level. The shear modulus of a beam is given by G_0 , and n is the material penalization parameter. In the present work the values of $G_0 = 1.0 \times 10^6$ and $n = 2$ will be used.

B. Distortional Rigidity Maximization

Distortion is an in-plane deformation of a beam section, and it is usually coupled with in-plane rigid-body rotation. Although distortional deformation is insignificant in solid sections, it cannot be neglected in thin-walled sections. Figure 1 shows the typical in-plane deformation of a thin-walled beam section subjected to a couple. The cross sections near the loaded tip go through significant deformation, which can be decomposed into in-plane distortional deformation and rigid-body rotation associated with torsion. Conventional beam theories predict rigid-body section rotations and shear stresses. However, distortional bending stresses along the contour of the beam cross section are also developed, which become more significant when beam walled are very thin. The importance and mechanics of the distortion in thin-walled beams are explained in Refs. 6 and 7, and the significant effects near joints of thin-walled beams are also discussed in Refs. 13 and 14.

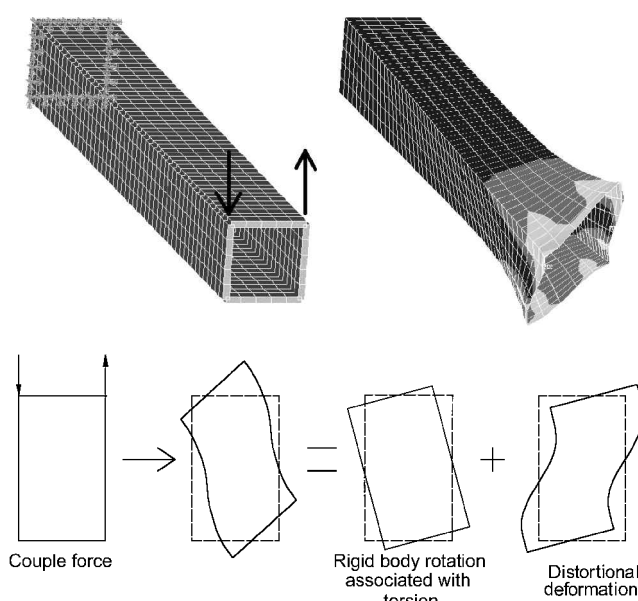


Fig. 1 Deformation of a thin-walled box beam under a couple.

Although the distortional stiffness in a thin-walled beam is explicitly given in Ref. 7, it has not been defined for general solid beams. Extending the notion of the distortional stiffness in Ref. 7, we propose to measure the distortional rigidity by means of the eigenvalue $\Lambda(\rho)$ of the following plane-strain problem:

$$^x KU = \Lambda(\rho)U \quad (7)$$

$$^x K = \sum_{e=1}^{N_e} \int_{A_e} {}^x B_e^T {}^x D(\rho_e) {}^x B_e \, dA \quad (8)$$

$${}^x D(\rho_e) = \frac{E(\rho_e)}{(1+\nu)(1-2\nu)} \begin{bmatrix} 1 & \nu & 0 \\ \nu & 1 & 0 \\ 0 & 0 & (1-2\nu)/2 \end{bmatrix} \\ E(\rho_e) = E_0 \left(\frac{\rho_e}{\rho_u} \right)^n \quad (9)$$

In Eq. (7) ${}^x K$ is the stiffness matrix of the plane-strain problem defined in the region occupied by a beam section, and U is the displacement vector. The element strain interpolation matrix is denoted by ${}^x B_e$, and Young's modulus of the beam is given by $E_0 = 2.6 \times 10^6$. To maximize the distortional rigidity of a beam section, the fundamental eigenvalue $\Lambda(\rho)$ of Eq. (7) will be maximized. This problem can be formulated in a topology optimization setting by replacing Eq. (1a) by

$$f(\rho) = -\Lambda(\rho) \quad (10)$$

The rest of Eq. (1) remains unchanged.

One of the serious problems in eigenvalue-related optimization problems is mode switching that usually causes discontinuity in the optimization process.¹⁵ Because the distortional rigidity is defined by an eigenvalue, the distortional mode must be tracked during the optimization process to prevent the discontinuity. In this work we utilize the Mac-based mode tracking method¹⁶ to overcome the discontinuity problem.

C. Sensitivity Analysis

The sensitivities of each function in Eqs. (1) and (10) with respect to the design variable ρ_e are the key information in updating the design variables. The procedure for the sensitivity analysis in structural optimization problems can be found in Ref. 17. Here, we summarize the results, briefly.

One can show that the sensitivities of the torsional and distortional rigidities in Eqs. (1a) and (10) can be written as

$$\frac{\partial D_t(\rho)}{\partial \rho_e} = -\Phi_e^T \frac{\partial \phi K_e}{\partial \rho_e} \Phi_e = \frac{n}{\rho_e} \Phi_e^T \phi K_e \Phi_e \quad (11)$$

$$\frac{\partial \Lambda(\rho)}{\partial \rho_e} = U_e^T \frac{\partial {}^x K_e}{\partial \rho_e} U_e = \frac{n}{\rho_e} U_e^T {}^x K_e U_e \quad (12)$$

The sensitivity of the mass constraint in Eq. (1b) is simply

$$\frac{\partial h(\rho)}{\partial \rho_e} = \int_{A_e} dA \quad (13)$$

III. Construction of a Multiobjective Function

It is important to realize the conflicting nature between the torsional rigidity optimization and distortional rigidity optimization. One can show that the solution of the topology optimization problem stated by Eq. (1) is a hollow thin-walled closed section when the mass constraint becomes tight. On the other hand, a tight mass constraint for the distortional rigidity optimization problem, stated by Eq. (10), yields a lumped mass concentrated at the center of a beam cross section.

To find an optimal beam section that maximizes both the torsional and distortional rigidities, one can construct a weighted sum of the rigidities as an objective function:

$$f_s = -(w_D D_t + w_\Lambda \Lambda) \quad (14)$$

where w_D and w_Λ are weighting factors. However, the use of such an objective function can result in solution divergence because the conflict in maximizing the rigidities is severe. To resolve this problem, we propose to use a multiobjective function in the following product form:

$$f_p = -\ln(D_t^{w_D} \Lambda^{w_\Lambda}) \quad (15)$$

The effects of the functional form of the objective functions can manifest themselves in the following sensitivity expressions:

$$\frac{\partial f_s}{\partial \rho_e} = -\left(w_D \frac{\partial D_t}{\partial \rho_e} + w_\Lambda \frac{\partial \Lambda}{\partial \rho_e}\right) \quad (16)$$

$$\frac{\partial f_p}{\partial \rho_e} = -\left(w_D \frac{\partial D_t / \partial \rho_e}{D_t} + w_\Lambda \frac{\partial \Lambda / \partial \rho_e}{\Lambda}\right) \quad (17)$$

Although the sensitivity $\partial f_p / \partial \rho_e$ is proportional to the normalized sensitivities of D_t and Λ , the sensitivity $\partial f_s / \partial \rho_e$ is proportional to the unnormalized sensitivities of D_t and Λ . Because of the normalization factors D_t and Λ appearing in the denominators of Eq. (17), the objective function f_p becomes less sensitive to the variations of D_t and Λ as D_t and Λ become larger, and vice versa. Furthermore, the normalization factors D_t and Λ serve to balance the effects of D_t and Λ on the sensitivity of the objective function f_p . More discussions on multiobjective formulation for topology optimization can be found in Refs. 18 and 19.

Instead of using multiobjective functions, one can optimize only one objective while all others are considered as constraint. However, it appears difficult to preselect the bounds of all constraints for the present problem.

IV. Updating Design Variables

An optimality criterion (OC) algorithm has generally been used in topology optimization problems because the OC algorithm is very effective in dealing with problems with very many design variables. The optimality criterion is very simple and intuitive compared to mathematical programming. In the present work the topology optimization problem is defined by Eqs. (1b), (1c), and (15). We set up an updating rule using the Kuhn–Tucker condition for these equations, although the same result can be obtained rigorously.²⁰

The Lagrangian function of the present optimization problem is stated as

$$L(\rho, \mu) = f(\rho) + \mu h(\rho) \quad (18)$$

For the stationary condition at the optimal point, the derivatives with respect to all variables must be zero:

$$\frac{\partial L}{\partial \rho_e} = \frac{\partial f}{\partial \rho_e} + \mu \frac{\partial h}{\partial \rho_e} = 0 \quad (19)$$

$$\frac{\partial L}{\partial \mu} = h = 0 \quad (20)$$

By introducing the index such that

$$\prod_e = -\frac{1}{\mu} \frac{\partial f / \partial \rho_e}{\partial h / \partial \rho_e} \quad (21)$$

Equation (19) can be written as $\prod_e = 1$. The updating rule in the OC algorithm is written as

$$\rho_e^{k+1} = \prod_e^\eta \rho_e^k \quad (22)$$

such that

$$h(\rho_e^{k+1}) = 0 \quad (23)$$

where η is a damping factor to control the convergence speed and k is the index representing the iteration number. In the updating rule in Eqs. (22) and (23), a proper move limit and the side constraints in Eq. (1c) must be considered. For more details see Refs. 9 and 17.

In topology optimization the checkerboard problem is a common difficulty caused from the instability of numerical analysis.^{10,11,21}

Among various schemes to prevent the checkerboard pattern, we employ the method of averaging adjacent element densities or sensitivities.²¹

V. Numerical Examples

A. Example 1: Square Design Domain

A square design domain for a beam section and its fundamental distortional deformation mode are depicted in Fig. 2. The objective function f_p of Eq. (15) is considered first, where the weighting

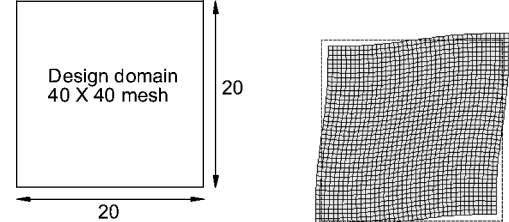


Fig. 2 Example 1: square design domain and its fundamental distortional mode.

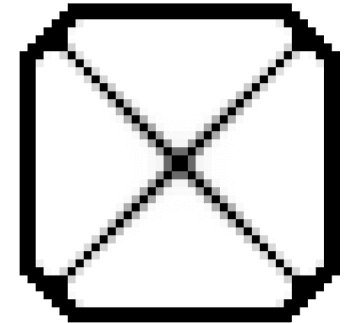
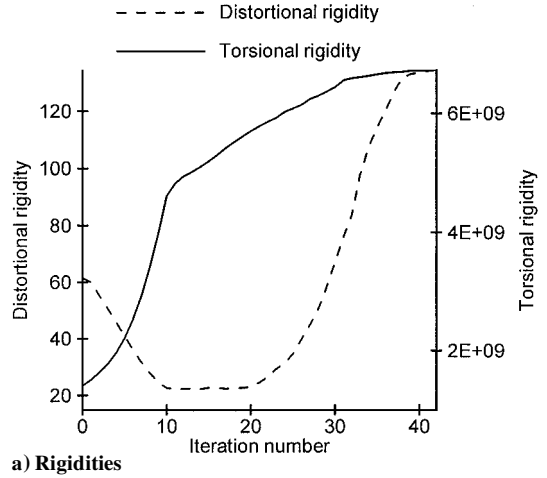


Fig. 3 Optimized result for example 1 ($f_p: w_D = 1.0, w_\Lambda = 0.01$).



a) Rigidities

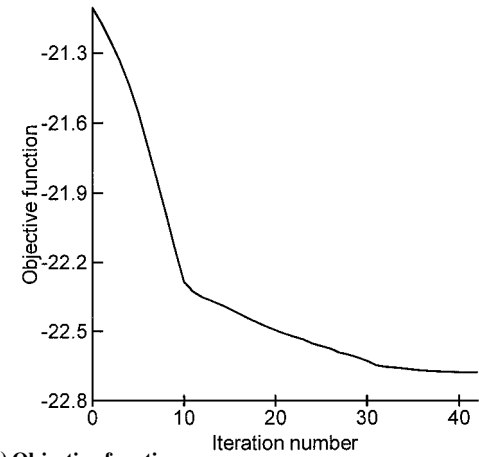
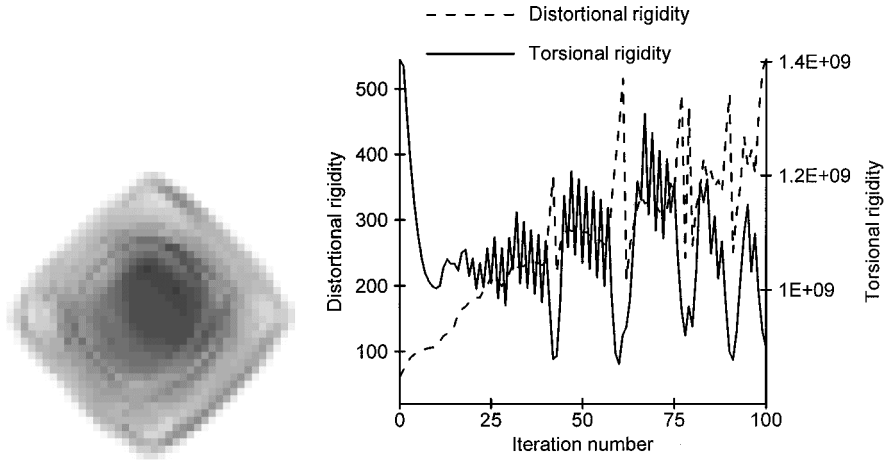
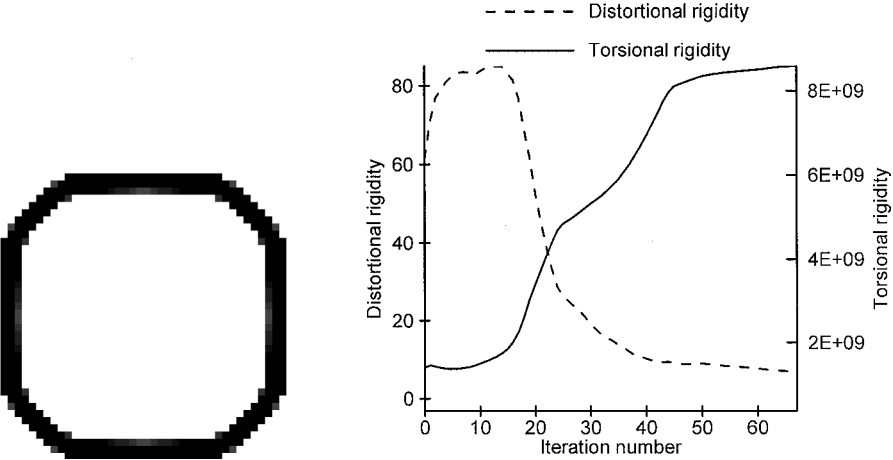


Fig. 4 Iteration history for example 1 ($f_p: w_D = 1.0, w_\Lambda = 0.01$).

Table 1 Numerical values of the torsional and distortional rigidities at the initial and final design iterations

Example	Torsional rigidity		Distortional rigidity		Objective function	
	Initial	Final	Initial	Final	Initial	Final
1, $f_p: w_D = 1.0, w_A = 0.01$	1.404e+9	6.731e+8	61.40	134.4	-21.10	-22.679
1, $f_s: w_D = 0.05, w_A = 1.0$	1.404e+9	0.8997e+9	61.40	544.8	-7.020e+7	-4.499e+7 (not optimized)
1, $f_s: w_D = 0.075, w_A = 1.0$	1.404e+9	8.593e+8	61.40	6.868	-1.053e+8	-6.445e+8
2, $f_p: w_D = 1.0, w_A = 0.005$	0.7809e+9	4.665e+9	11.82	45.90	-20.49	-22.28
3, $f_p: w_D = 1.0, w_A = 0.0$	0.6250e+9	1.931e+9	24.35	22.68	-20.25	-21.38
3, $f_p: w_D = 1.0, w_A = 0.01$	0.6250e+9	1.860e+9	24.35	89.89	-20.29	-21.39
3, $f_p: w_D = 1.0, w_A = 0.05$	0.6250e+9	1.647e+9	24.35	101.5	-20.41	-21.45

**Fig. 5** Results for example 1 ($f_s: w_D = 0.05, w_A = 1.0$).**Fig. 6** Results for example 1 ($f_s: w_D = 0.075, w_A = 1.0$).

factors are taken as $w_D = 1.0$ and $w_A = 0.01$. As mentioned in the preceding section, the distortional mode in Fig. 2 is tracked during the optimization process to avoid the discontinuity in the sensitivity calculations.¹⁶ Figure 3 shows the optimized results with a 25% mass constraint. The initial design starts with a uniform density distribution of $\rho_e = 0.25$.

As shown in Fig. 3, a hollow diagonally stiffened thin-walled section is obtained. The stiffened section obtained in Fig. 3 is indeed a typical section employed to suppress distortional deformation.²² In practical applications the stiffening is accomplished by spacing appropriately the transverse ribs indicated in Fig. 3.

The histories of the rigidities and the objective function are plotted in Fig. 4. In Fig. 4a the conflicting nature of the rigidities is clearly shown, particularly at the initial design stage. The numerical values of the torsional and distortional rigidities for all examples considered in this work are summarized in Table 1.

To investigate the advantage of the objective function f_p in Eq. (15) over f_s in Eq. (14), we also consider a beam-section de-

sign problem with the objective function f_s . Figures 5 and 6 show the results with different weighting factors. Because the weighting factor for the distortional rigidity is larger than that for the torsional rigidity, only the distortional rigidity is increased while the torsional rigidity experiences many oscillations as shown in Fig. 5. Moreover, the optimized shape of the cross section in Fig. 5 has no physical meaning. A slight increase in the weighting factor for the torsional rigidity results in a hollow section without any reinforcement as shown in Fig. 6. The value of the distortional rigidity is even reduced when it is compared with the initial value.

The weighting factors w_D and w_A have been determined by numerical experiments, and their effects on results are illustrated in Fig. 7. The performance of the objective function f_p is superior to that of the typical objective function f_s . As shown in Fig. 7b, the use of f_s does not yield any useful section that resists effectively torsion and distortion. However, the use of the present objective function f_p can yield a section well known to resist distortion. Though no rigorous approach to select the weighting factors for f_p is provided,

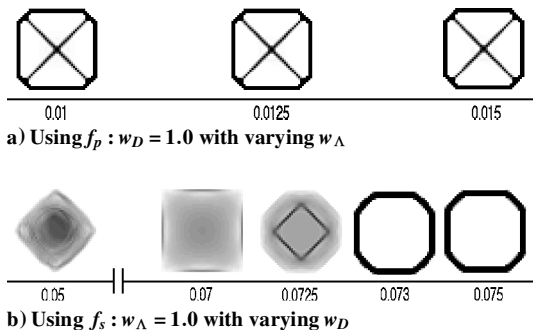


Fig. 7 Optimized results with varying weighting factors.

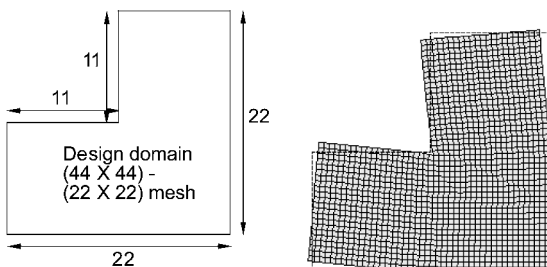


Fig. 8 L-shaped design domain and its fundamental distortional mode.

Fig. 9 Optimized result for example 2 ($f_p: w_D = 1.0, w_A = 0.005$).

the present multiobjective function f_p is shown to yield satisfactory results.

B. Example 2: L-Shaped Design Domain

An L-shaped design domain and its distortional deformation mode are depicted in Fig. 8. The values of initial design variables ρ_e are uniform with $\rho_e = 0.25$, and a 25% mass constraint is used. The optimal beam-section configuration obtained with f_p in Eq. (15) is shown in Fig. 9. In beam sections having concave shapes like an L-shaped section, one can appreciate the importance of the inclusion of the distortional rigidity in the objective function.

C. Example 3: Reinforcement of a Trapezoidal Thin-Walled Section

As the final example, we consider a reinforcing problem of a trapezoidal thin-walled beam section in which both the torsional and distortional rigidities are to be increased. By using different sets of weighting factors, reinforcements are expected to have different shape and topology. The design domain and its fundamental distortional deformation pattern are depicted in Fig. 10. The trapezoidal thin-walled beam is a practical structural member used in many engineering applications. The optimized results shown in Fig. 11 are obtained with $(w_D = 1.0, w_A = 0.0)$, $(w_D = 1.0, w_A = 0.01)$, and $(w_D = 1.0, w_A = 0.05)$, respectively. Here, the values of the initial design variables ρ_e are uniform with $\rho_e = 0.15$, and a 15% mass constraint is used. The use of higher values of w_A in this trapezoidal section tends to in-

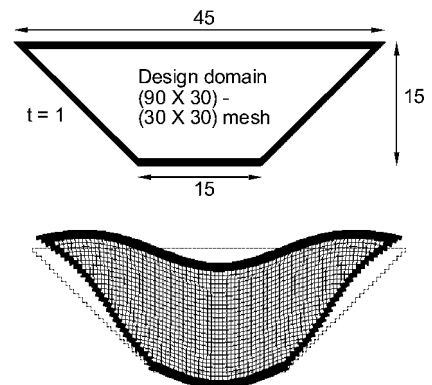


Fig. 10 Trapezoidal design domain and its fundamental distortional mode.

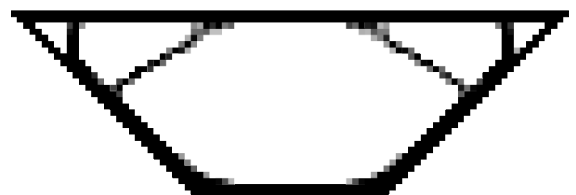
a) Using f_p with $w_D = 1.0, w_A = 0.0$ (torsional rigidity only)b) Using f_p with $w_D = 1.0, w_A = 0.01$ c) Using f_p with $w_D = 1.0, w_A = 0.05$

Fig. 11 Optimized result for example 3.

crease the number of stiffening ribs, which stiffen its distortional rigidity.

VI. Conclusions

Thin-walled beam-section design to maximize the torsional and distortional rigidities was carried out in the frame of multiobjective topology optimization. The present multiobjective function in product form was shown to handle effectively multiobjective design problems in which the nature of objectives involved is seriously conflicting. The role of the distortional rigidity was revealed through several examples. The fundamental eigenvalue of the in-plane stiffness matrix for a section served well to define the distortional rigidity.

Acknowledgment

This work was supported by the Brain Korea 21 Project.

References

- 1 Banichuk, N. V., and Karihaloo, B. L., "Minimum-Weight Design of Multipurpose Cylindrical Bars," *International Journal of Solids and Structures*, Vol. 12, No. 2, 1976, pp. 267-273.
- 2 Parbery, R. D., and Karihaloo, B. L., "Minimum-Weight Design of Hollow Cylinders for Given Lower Bounds on Torsion and Flexural Rigidities," *International Journal of Solids and Structures*, Vol. 13, No. 8, 1977, pp. 1271-1280.

³Mota Soares, C. A., Rodrigues, H. C., and Oliveira Faria, L. M., "Optimization of Shafts Using Boundary Elements," *Journal of Mechanisms, Transmissions and Automation in Design*, Vol. 106, No. 2, 1984, pp. 199-202.

⁴Gracia, L., and Doblare, M., "Shape Optimization of Elastic Orthotropic Shafts Under Torsion by Using Boundary Elements," *Computers and Structures*, Vol. 30, No. 6, 1988, pp. 1281-1291.

⁵Kim, Y. Y., and Kim, T. S., "Topology Optimization of Beam Cross Sections," *International Journal of Solids and Structures*, Vol. 37, No. 4, 2000, pp. 477-493.

⁶Kim, Y. Y., and Kim, J. H., "Thin-Walled Closed Box Beam Element for Static and Dynamic Analysis," *International Journal for Numerical Methods in Engineering*, Vol. 45, No. 4, 1999, pp. 473-490.

⁷Kim, J. H., and Kim, Y. Y., "One Dimensional Analysis of Thin-Walled Closed Beams Having General Cross Sections," *International Journal for Numerical Methods in Engineering*, Vol. 49, No. 5, 2000, pp. 653-668.

⁸Timoshenko, S. P., and Goodier, J. N., *Theory of Elasticity*, 3rd ed., McGraw-Hill, New York, 1970, pp. 291-353.

⁹Bendsøe, M. P., and Kikuchi, N., "Generating Optimal Topologies in Structural Design Using a Homogenization Method," *Computer Methods in Applied Mechanics and Engineering*, Vol. 71, No. 2, 1988, pp. 197-224.

¹⁰Bendsøe, M. P., and Mota Soares, C. A., *Topology Design of Structures*, Kluwer Academic, Norwell, MA, 1993, pp. 287-300.

¹¹Bendsøe, M. P., *Optimization of Structural Topology, Shape, and Material*, Springer-Verlag, Berlin, 1995, pp. 5-77.

¹²Bendsøe, M. P., and Sigmund, O., "Material Interpolation Schemes in Topology Optimization," *Archive of Applied Mechanics*, Vol. 69, No. 9, 1999, pp. 635-654.

¹³Kim, Y. Y., Yim, H. J., Kang, J. H., and Kim, J. H., "Reconsideration of the Joint Modeling Technique: in a Box Beam T-Joint," Society of Automotive Engineers, 951108, 1995, pp. 275-279.

¹⁴Balch, C. D., and Steele, C. R., "Asymptotic Solution for Warping and Distortion of Thin-Walled Box Beams," *Journal of Applied Mechanics*, Vol. 54, No. 2, 1987, pp. 165-173.

¹⁵Eldred, M. S., Venkayya, V. B., and Anderson, W. J., "Mode Tracking Issues in Structural Optimization," *AIAA Journal*, Vol. 33, No. 10, 1995, pp. 1926-1933.

¹⁶Kim, T. S., and Kim, Y. Y., "Mac-Based Mode Tracking in Structural Topology Optimization," *Computers and Structures*, Vol. 74, No. 3, 2000, pp. 375-383.

¹⁷Haftka, R. T., and Gürdal, Z., *Elements of Structural Optimization*, 3rd ed., Kluwer Academic, Norwell, MA, 1992, pp. 255-304.

¹⁸Ma, Z. D., Kikuchi, N., and Cheng, H. C., "Topological Design for Vibrating Structures," *Computer Methods in Applied Mechanics and Engineering*, Vol. 121, No. 3, 1995, pp. 259-280.

¹⁹Nishiawaki, S., Frecker, M. I., Min, S., and Kikuchi, N., "Topology Optimization of Compliant Mechanisms Using the Homogenization Method," *International Journal for Numerical Methods in Engineering*, Vol. 42, No. 3, 1998, pp. 535-559.

²⁰Ma, Z. D., Kikuchi, N., and Hagiwara, I., "Structural Topology and Shape Optimization for a Frequency Response Problem," *Computational Mechanics*, Vol. 13, No. 2, 1993, pp. 157-174.

²¹Sigmund, O., and Petersson, J., "Numerical Instabilities in Topology Optimization: a Survey on Procedures Dealing with Checkerboards, Mesh-Independencies and Local Minima," *Structural Optimization*, Vol. 16, No. 1, 1998, pp. 68-75.

²²Heins, C. P., *Bending and Torsional Design in Structural Members*, Lexington Books, Lexington, KY, 1975.

A. Chattopadhyay
Associate Editor